

Intramolecular Proton-Transfer Processes Starting at Higher Excited States: A Fluorescence Study on 2-Butylamino-6-methyl-4-nitropyridine *N*-Oxide in Nonpolar Solutions

Joost S. de Klerk,[†] Anna Szemik-Hojniak,[‡] Freek Ariese,^{*,†} and Cees Gooijer[†]

Analytical Chemistry & Applied Spectroscopy, Laser Centre Vrije Universiteit Amsterdam, De Boelelaan 1083, 1081 HV Amsterdam, The Netherlands, and Faculty of Chemistry, University of Wrocław, ul. F. Joliot-Curie 14, 50-383 Wrocław, Poland

Received: November 5, 2006; In Final Form: April 4, 2007

This article describes the exceptional photophysics of 2-butylamino-6-methyl-4-nitropyridine *N*-oxide (2B6M). It is known from the literature that this compound may undergo excited-state intra- or intermolecular proton-transfer reactions. In nonpolar solvents, 2B6M exhibits an unusual fluorescence behavior: there is a substantial difference between the relative band intensities of the excitation and absorption spectra. Furthermore, in emission two bands are observed, and their relative intensities depend on the excitation wavelength, thus violating the Kasha–Vavilov rule. It is the objective of this research to interpret these results. For this purpose, steady-state fluorescence excitation and emission spectra in the liquid state were recorded and quantum yields were determined for the two types of emission. In addition, absorption spectra were measured at room temperature and under low-temperature conditions. Finally, fluorescence lifetimes of the emitting species were determined using the time-correlated single photon counting technique. The results suggest that in the liquid state only one (monomeric) ground state species dominates, which can emit via two different pathways (from the normal and the tautomeric excited state). The excitation spectra point at two different internal proton-transfer processes, one starting at the S_1 state and one starting at the S_2 state. On the basis of the measured lifetimes and fluorescence quantum yields, a kinetic scheme was completed that can quantitatively explain the observations.

1. Introduction

Pyridine *N*-oxide derivatives constitute a class of compounds that are widely studied in various chemical disciplines, especially in photochemistry and biochemistry. They may exhibit valuable physical properties such as efficient second-harmonic generation of electromagnetic radiation. An example is 3-methyl-4-nitropyridine-1-oxide, which is one of the best electrooptical materials in the visible region.¹ Furthermore, these compounds are widely used in organic chemistry as synthetic intermediates, protecting groups, auxiliary agents, oxidants, ligands in metal complexes, and catalysts.² In biochemistry, the 4-nitropyridine *N*-oxide derivatives are especially interesting because of their exceptionally high bioactivity. It has been stated that the change of the electronic system induced by the nitro group is critical in this respect.³

The subclasses nitramino pyridine *N*-oxides (NAPNO) and alkylamino nitropyridine *N*-oxides (AANPNO) are of particular interest because they may undergo both intra- and intermolecular proton transfer.^{4–6} As commonly known, the photoexcitation of such molecules leads to drastic changes of their acid–base properties with respect to the ground state. Molecules giving rise to excited-state tautomers by intramolecular proton-transfer reactions (ESIPT) have attracted considerable attention from both an experimental and a theoretical point of view.^{7–11} The intermolecular and specifically the excited-state double proton-

transfer reactions are interesting because of the possibility to imitate the mechanism of photomutagenesis in DNA.^{12–15}

Concerning the AANPNOs, the spectroscopic literature has mainly focused on one particular representative, that is, 2-butylamino-6-methyl-4-nitropyridine *N*-oxide (2B6M; Figure 1) in aprotic polar solvents such as acetonitrile.¹⁶ In the crystal structure of 2B6M, dimers that may be formed via a double hydrogen bond between the hydrogens of the amino groups and the oxygen atoms of the NO groups are also observed.¹⁷ The probability of dimerization may of course be very different in solution. It is critical to find out whether monomers and dimers of 2B6M could be present simultaneously in liquid nonpolar solutions at room temperature. In a recent article,¹⁷ it was suggested that exclusively dimers are present. This conclusion was based on the temperature influence (although minor) on the absorption spectra in the range from 25 to 80 °C. Differences in the spectra were interpreted as an indication for two dimer forms (i.e., stacked ones and doubly hydrogen-bonded ones). However, more solid experimental evidence is required to draw unambiguous conclusions.

In nonpolar solutions (*n*-octane), we observed an interesting spectroscopic behavior: the relative band intensities in the (corrected) fluorescence excitation and absorption spectra do not properly match. The same was also observed in cyclohexane by another research group,¹⁶ but thus far no satisfactory explanation was provided. In emission, two bands are observed and their relative intensities depend on the excitation wavelength. At first sight, the results would suggest that, in nonpolar solvents, not only in the excited state but also in the ground state more species might coexist. However, the experimental

* Corresponding author. Telephone: +31 20 5987524. Fax: +31 20 5987543. E-mail: ariese@few.vu.nl.

[†] Laser Centre Vrije Universiteit Amsterdam.

[‡] University of Wrocław.

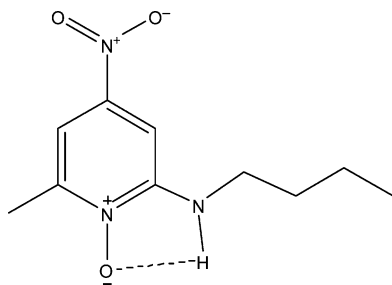


Figure 1. Molecular structure of 2B6M showing intramolecular H-bonding.

findings described in this article indicate that in the ground state a single, monomeric species exists and that complex excited-state processes provide a more likely explanation. For this work, absorption, low-temperature absorption, and steady-state fluorescence excitation and emission spectra were recorded. Fluorescence lifetime measurements were determined using time-correlated single-photon counting.

2. Experimental Section

2.1. Chemicals. The synthesis of 2B6M is described in ref 16. All measurements were done using solutions with different concentrations of 2B6M in *n*-octane (Aldrich anhydrous grade, purity >99%). The purity of 2B6M was checked using GC/MS using a 30-m DB5MS column (J&W Scientific, Folsom, CA), scan range *m/z* 35–350.

2.2. Absorption and Fluorescence, Room Temperature. The absorption spectra at room temperature were measured with a Cary 50 Conc spectrophotometer (Varian, Palo Alto, CA) with a spectral bandwidth of 1.5 nm, using 1-, 10-, and 40-mm quartz absorption cuvettes. The fluorescence excitation and emission spectra were recorded using a luminescence spectrometer LS-50B (Perkin-Elmer, Waltham, MA) with a 10-mm fluorescence quartz cuvette at a scan speed of 100 nm/min. The spectral bandwidths in excitation and emission were typically 7.5 and 12.5 nm, respectively, for the excitation measurements and conversely for the emission measurements. For the measurements, cutoff filters of 430 or 515 nm were inserted into the emission path, depending on the emission range of interest. Blank spectra (solvent impurities and Raman) were subtracted, taking into account the excitation inner filter effect at higher concentrations. For the excitation spectra, the maximum absorbance value (at 407 nm) was 0.04 over a path length of 5 mm to the center of the cuvette. Spectra were corrected for the differences in excitation intensity (reference photomultiplier) and detector sensitivity.

For the quantum yield experiments, emission spectra were recorded using a Spex Fluorolog spectrofluorimeter (Spex Ind., Edison, NJ), applying excitation correction, emission correction, and correction for losses in the 5×10^{-5} M 2B6M sample as a result of the excitation inner filter effect (taking a 5-mm path length to the center of the cuvette). The spectral bandwidths in excitation and emission were 10 and 4 nm, respectively. Fluorescence quantum yields were determined at two wavelengths by quantitative comparison of the absorption and the emission spectra of 2B6M with those of the reference fluorophore perylene in cyclohexane (concn 10^{-7} M at 333 nm and 10^{-8} M at 407 nm), which has a quantum yield of 0.94.¹⁸ The extinction coefficients were originally derived from the absorption spectra, measured with a fixed bandwidth of 1.5 nm. Later measurements with broader slits confirmed that with a 10-nm bandwidth (as applied for the fluorescence quantum yield

measurements) the extinction coefficients of 2B6M and perylene were not significantly different at 333 and 407 nm.

2.3. Fluorescence Lifetime Measurements. For time-correlated single-photon counting experiments, an SPC-630 (Becker & Hickl GmbH, Berlin, Germany) system with a time resolution of about 8 ps was used. A reflection of the laser pulse on a photodiode provided the synchronization signal. The laser system consisted of a Mira 900-P (Coherent, Santa Clara, CA) laser, emitting 3-ps pulses at a repetition rate of 76 MHz, pumped by a Verdi V8 diode-pumped solid-state laser (Coherent). The laser emission (tuned to 800 nm) was led through a pulse picker model 9200 (Coherent), which reduced the repetition rate to 3.8 MHz to avoid excitation by a previous pulse. A frequency doubler model 5-050 (Inrad, Northvale, NJ) was used to provide the final output wavelength of 400 nm, exciting the sample in a quartz cuvette with 1-cm path length. Fluorescence emission was collected at an angle of 90°, dispersed by a monochromator (TVC JarrellAsh Monospec 18, Grand Junction, CO), and detected by a microchannel plate photomultiplier tube (Hamamatsu, Shimokanzo, Japan). The instrument response function was obtained from a solvent Raman line and had a fwhm of about 30 ps. Lifetimes were obtained by deconvolution of the decay curves using the FluoFit software program (PicoQuant GmbH, Berlin, Germany). All lifetimes were fitted to a χ^2 value of less than 1.2 and with a residuals trace that was fully symmetrical around the zero axis. Decays were recorded at wavelengths between 460 and 630 nm.

2.4. Low-Temperature Absorption Measurements. For the low-temperature absorption measurements, a homemade absorption setup was designed. The sample holder consisted of two cells (with a 7-mm diameter and 5-mm optical path with sapphire windows on both sides) to be used for the sample and the solvent blank, respectively. The samples were cooled by a Cryodine 21 closed-cycle helium refrigerator (CTI Cryogenics, Waltham, MA), which could be operated over a temperature range of 293–12 K. The light source was a model 5000XeF xenon flash lamp (IBH, Glasgow, U.K.), and detection was performed with an optical fiber and a PC2000 PC plug-in spectrometer (Ocean Optics, Dunedin, FL). The spectra were corrected for lamp profile and background scatter by consecutive measurements of the sample and the blank. This way, absorption spectra were obtained at different temperatures with a resolution of about 2 nm.

3. Results

To investigate whether monomers and dimers could be present simultaneously, *molecular absorption spectra* of 2B6M in *n*-octane at room temperature were measured at seven different concentration levels and furthermore over a temperature range from room temperature down to 240 K, still above the solidification point of *n*-octane. As expected, the spectra in *n*-octane were quite similar to that measured in cyclohexane by Poór et al.¹⁶ The absorption maxima, spectral shapes, and relative intensities of the bands did not change as a function of concentration. The room-temperature spectra are shown in Figure 2; their similarity indicates that there is no concentration dependency over the range 5×10^{-7} to 1×10^{-3} M (a 2000-fold change in 2B6M concentration).

The lack of concentration dependence observed in liquid *n*-octane solutions indicates that either dimerization is negligible so that exclusively the monomer is observed, or only the dimer is observed if its dissociation were fully negligible even at a 2B6M concentration as low as 5×10^{-7} M. The second option would require an extremely stable complex with a dimer

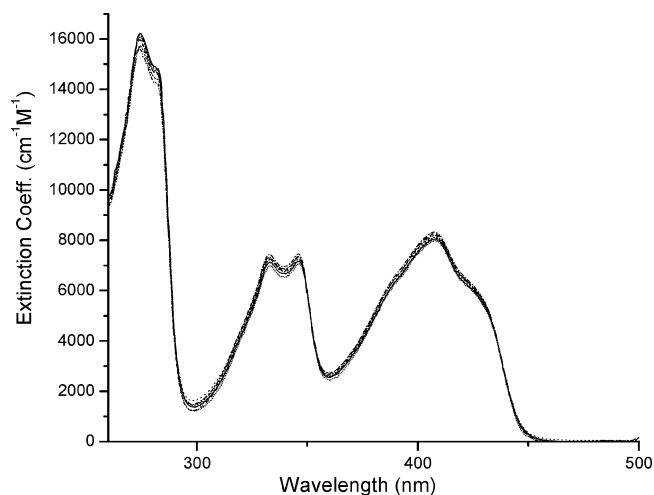


Figure 2. Absorption spectra of 2B6M in *n*-octane at seven different concentrations ranging from 5×10^{-7} to 1×10^{-3} M; path length: 4.0 cm (lowest two concentrations), 1.0 cm (intermediate concentrations), and 0.1 cm (highest concentration).

dissociation constant of the order of 10^{-10} M or smaller, which seems to be quite unlikely (for instance, the dimer dissociation constant of 7-azaindole in carbon tetrachloride is 8.5×10^{-3} M).¹⁹ Therefore, we conclude that in the ground state under the conditions at hand (liquid, alkane solution) only the monomeric species is present.

Also, a temperature decrease from 293 to 240 K did not result in any significant spectral change (not shown). It is reasonable to assume that the absorption spectra of a dimer and a monomer would be substantially different. At 200 K (upon solidification of the solution), such changes were observed indeed: a broad band appeared in the 450–500 nm range, pointing at the presence of a new species such as a dimer. It is not unexpected that upon solidification of *n*-octane associate formation is stimulated, especially if monomers with strong polar or charged groups are dealt with or as in this case the molecule contains both a hydrogen bond donor and a hydrogen bond accepting group. These findings also indicate that in the liquid state we are dealing with a monomeric species. Absorption spectra under cryogenic conditions will be discussed in more detail in a forthcoming article.

It should be noted that the presence of more than one conformational isomer (for instance, rotameric forms of the alkylamino group) of 2B6M might still be possible, since these cannot be distinguished in the above experiments. The most favorable structure of the 2B6M monomer (R_1 , shown in Figure 1) indicates the possibility of an intramolecular N–H···O hydrogen bridge.¹⁷

Fluorescence excitation and emission spectra recorded at room temperature are complex. The (corrected) emission spectra are composed of more than one band (Figure 3). The major one shows peaks/shoulders at 452 and 471 nm. Furthermore, weaker emissions of 545, 595, and 642 nm can be seen. Both types of emission are rather weak and show short, subnanosecond lifetimes (no phosphorescence was observed). Surprisingly, the relative intensities of the emission bands depend on the excitation wavelength.

At first sight, the existence of two emission bands seems to be straightforward in view of the available information on the behavior of 2B6M in the excited state:¹⁶ after excitation, the normal form (N^*), emitting in the blue at 452/471 nm, can undergo ESIP so that a tautomeric form (T^*) is created, emitting in the yellow range at 545 nm and longer. In

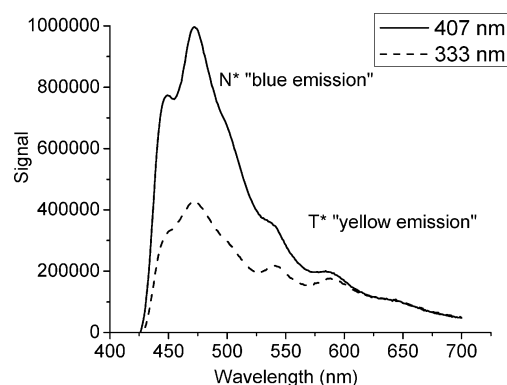


Figure 3. Emission spectra of 2B6M in *n*-octane at a concentration of 5×10^{-5} M at room temperature. The excitation wavelengths are 333 nm (dashed line) and 407 nm (full line).

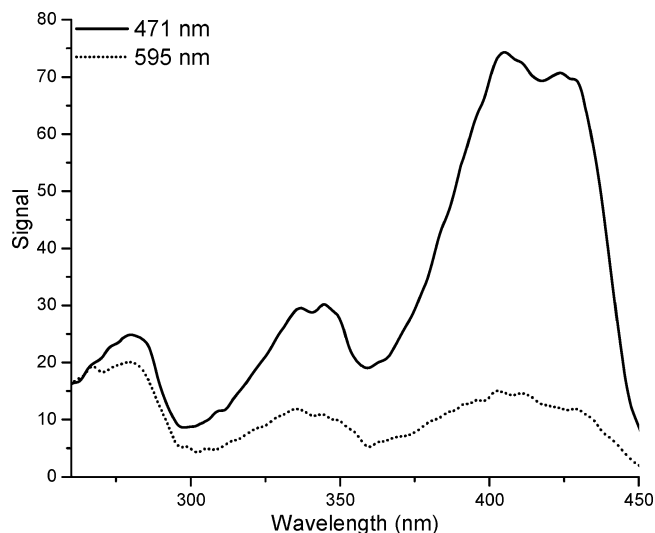


Figure 4. Excitation spectra of 2B6M in *n*-octane at a concentration of 1×10^{-5} M at room temperature. The emission was detected at the maxima of the emission spectra: 471 nm (full line) and 595 nm (dashed line).

acetonitrile, this proton-transfer process was studied in detail by Poór et al., using transient absorption spectroscopy,¹⁶ and a similar process could occur in nonpolar solvents. In acetonitrile, exclusively T^* is observed because of an extremely fast proton-transfer rate (10^{13} s⁻¹), with which N^* fluorescence cannot compete. The fact that in our experiments two types of emission are detected would indicate that in nonpolar solvents proton transfer is much slower so that the fluorescence quantum yield of N^* is no longer negligible.

However, this scheme alone cannot explain that the relative intensities of the two emission bands depend on the excitation wavelength. Also, one would expect the excitation spectrum to be identical with the absorption spectrum in Figure 2. Instead, the (corrected) excitation spectra in Figure 4 show obvious differences that depend on the emission wavelength monitored. Specifically, the relative intensities of the bands at about 280/333 nm and the one at 407 nm differ considerably. Only in the case of the excitation spectrum of the yellow emission at 595 nm do the relative intensities of the three bands match the absorption spectrum. The shapes of the bands differ slightly from those in absorption because of the low fluorescence intensity (noise) and the difference in spectral bandwidth. The observations were supported by similar spectra obtained at a higher concentration (not shown); at the 5×10^{-5} M level the spectra are less noisy but the excitation inner filter effect was no longer negligible.

TABLE 1: Fits of the Fluorescence Lifetimes of 2B6M Dissolved in *n*-Octane to a Mono- or Biexponential Function Convolved with the Instrument Response^a

emission wavelength (nm)	τ_1 (ps)	a_1 (counts)	τ_2 (ps)	a_2 (counts)
460	15 ± 5	339000		
470	13 ± 5	252000		
500	16 ± 5	152000		
545	17 ± 5	31000	103 ± 10	3300
590			95 ± 10	5200
630			97 ± 10	1500

^a The excitation wavelength was 400 nm. Only the fluorescence intensity decay at 545 nm required fitting with a biexponential function $I(\lambda, t) = a_1(\lambda) \exp[-t/\tau_1(\lambda)] + a_2(\lambda) \exp[-t/\tau_2(\lambda)]$.

At first sight, these differences would indicate the presence of a second species. However, as already discussed, dimer formation does not play a role. Such a species does not show up in the absorption spectra upon changing the concentration 2000-fold or lowering the temperature to 240 K. Furthermore, fluorescent solvent impurity is ruled out (except for solvent Raman, blank emission was negligible at 2B6M wavelengths). The only option would be another rotamer of 2B6M (rotation of 180° around the aryl-amino bond), denoted as R₂. One would expect similar, but not identical, absorption spectra for R₁ and R₂, whereas for R₂ the N* → T* transition would be inhibited because of the large distance to be overcome in case of proton transfer. This could explain a significant difference in emission for R₁ and R₂, but, however, not in excitation. To explain the differences in the excitation spectra (the band positions remaining the same, but their relative intensities changing), a species would be needed that (i) emits (almost) exclusively at 452/471 nm, that (ii) can be much more efficiently excited at 407 nm than at 280/333 nm, and that (iii) has a much higher fluorescence quantum yield than the species emitting at longer wavelength. We conclude that in view of the expected similarity of the absorption spectra and the observed fluorescence lifetimes (see the following paragraphs), the presence of a rotameric form R₂ cannot account for the observations in excitation shown in Figure 4.

Fluorescence quantum yields of the two emission types were determined at two wavelengths on the basis of comparison of the integrated emission with that of perylene. For the yellow T* emission, φ_T was found to be 1.5×10^{-4} , with no significant dependence on the excitation wavelength. For the blue N* emission, we obtained $\varphi_N = 6.0 \times 10^{-4}$ when exciting at 407 nm, but only 2.8×10^{-4} at $\lambda_{\text{ex}} = 333$ nm.

Fluorescence lifetimes of 2B6M in *n*-octane measured at room temperature are shown in Table 1. The fluorescence lifetime of the normal form N* (emission measured at 460, 470, and 500 nm) is very short, about 15 ps, which is of the same order as the instrument response function. The fluorescence lifetime of the tautomer T* (emission at 590 and 630 nm) is about 100 ps. At 545 nm, both emissions overlap and a biexponential function was needed to fit the decay. The error in τ_2 is larger because of the low fluorescence intensity of the T*. The short N* lifetime supports the assumption of fast proton transfer (see Discussion).

4. Discussion

Even though the absorption spectra indicate that in liquid *n*-octane only a single monomeric species exists, the fluorescence results show a complex excitation behavior: excitation into the first excited state S₁ leads to a higher ratio of N*/T*

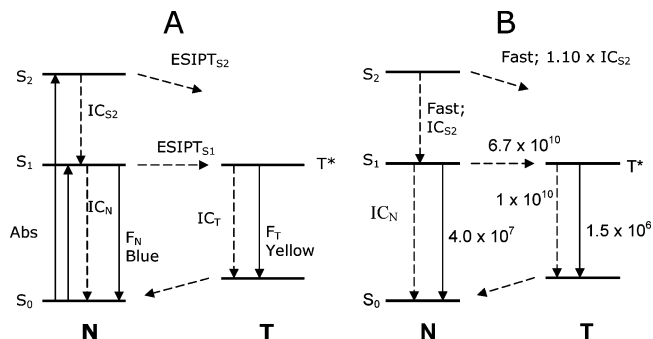


Figure 5. (A) Excited-state processes in 2B6M. (B) Corresponding rate constants (in s⁻¹) as derived in this work. Solvent, *n*-octane; room temperature.

(blue/yellow) emission than excitation into a higher state. The fluorescence quantum yield of the N* emission is not independent of the excitation wavelength, in violation of the Kasha–Vavilov rule.²⁰ The observations can be explained if we assume that ES IPT can also take place starting from the S₂ state (ES IPT_{S2}) and at a rate that can compete with the rate of internal conversion S₂ → S₁ (IC_{S2}). The various processes are illustrated in Figure 5A. The rate constants in this scheme can be inferred from the experimental results in the following way:

We note that the (corrected) excitation spectrum of the yellow T* emission is not significantly different from the absorption spectrum. Specifically, the relative intensities of the 333- and 407-nm bands in the lower spectrum of Figure 4 agree quite well with the difference in ϵ values from the absorption spectra of Figure 2 (7400 vs 8200 M⁻¹ cm⁻¹). This means that in the scheme of Figure 5 almost all excited molecules must end up in the T* state (irrespective of the excitation wavelength) and that therefore ES IPT_{S1} must be significantly higher than the rates of F_N and IC_N combined. On the other hand, the fact that blue emission is still observed means that F_N cannot be totally negligible compared to ES IPT_{S1}. Also, the intensities of the blue and yellow emission bands can only be rationalized if the fluorescence quantum yield of N* (in spite of the ES IPT_{S1} process) is still higher than that of T*.

The excitation spectrum of the blue N* band, however, shows an anomalous 407/333 band ratio of 2.33 instead of the 1.11 ratio in absorption. In other words, excitation into the S₁ state has a 2.10 times higher probability of leading to blue N* emission than excitation into the S₂ state. This can be explained by the model if at higher excited states the quantum yield of internal conversion reflects that same ratio: IC_{S2}/(ES IPT_{S2} + IC_{S2}) = 1/2.10 = 0.48. Neither IC_{S2} nor ES IPT_{S2} is currently known (probably of the order of 10¹³ s⁻¹), but the two processes are almost equally fast. Future femtosecond transient absorption measurements may shed light on the rates of these processes.

The fluorescence lifetimes in combination with φ_N , the fluorescence quantum yield of N* (upon excitation in the S₁ band), provide further clues as to the various rate constants. As listed in Table 1, $F_N + IC_N + ES IPT_{S1} = \tau_N^{-1} = 6.7 \times 10^{10}$ s⁻¹. As argued earlier, ES IPT_{S1} is by far the largest of the three components. Since $\varphi_N = F_N/(F_N + IC_N + ES IPT_{S1}) = 6.0 \times 10^{-4}$, F_N must be 4.0×10^7 s⁻¹. Similarly, $F_T + IC_T = \tau_T^{-1} = 1 \times 10^{10}$ s⁻¹. From $\varphi_T = 1.5 \times 10^{-4}$, it is calculated that F_T = 1.5×10^6 s⁻¹ and IC_T = 1×10^{10} s⁻¹. It should be mentioned that the nonradiative decay of N* and T* (indicated in Figure 5 as IC_N and IC_T) may in fact also include intersystem crossing (ISC). ISC is known to be important for many nitro compounds.²¹

Figure 5B shows the various rate constants derived for 2B6M in nonpolar solutions, as far as they could be determined from the experimental data at hand. Of the two competing processes at higher excited states, IC_{S_2} and $ESIPT_{S_2}$, only the ratio is known. This scheme can fully explain the experimental data observed for this molecule. The most exciting aspect of this figure is that *two* relevant pathways exist for ESIPT. The proton-transfer rate operational at the higher excited state S_2 must be competitive with internal conversion IC_{S_2} . Such high proton-transfer rates are not unlikely since they have been observed in several systems, including $ESIPT_{S_1}$ for 2B6M in acetonitrile.¹⁶ On the other hand, in *n*-octane solutions the ESIPT process in the S_1 state must be significantly slower (much slower than ESIPT in acetonitrile), otherwise the N^* state would be completely quenched and no blue fluorescence would occur. Quantum chemical calculations of the two tautomeric forms were carried out for the S_0 and S_1 states in a gas phase, hexane, and acetonitrile environment.¹⁷ Those calculations indeed predict a somewhat higher level of the T^* state in a nonpolar solvent as compared to acetonitrile, which would agree with a slower $ESIPT_{S_1}$ rate. The latter is crucial: only specific combinations of rate constants can result in the dual emission and their peculiar intensity ratios observed for 2B6M in nonpolar solvents.

5. Conclusion

From the present study, we can conclude that at room temperature 2B6M exists as a monomer in the nonpolar solvent *n*-octane. Only a single ground-state species is present, presumably with a predominant configuration as shown in Figure 1. The latter allows an efficient ESIPT reaction. Two emission bands are observed, one related to the normal configuration and one related to the tautomeric species after ESIPT. The relative ratios of the two emission bands depend on the excitation wavelength: the blue N^* emission is relatively strong upon excitation into the S_1 state and weaker upon excitation into a higher state. Apparently, for this molecule in a nonpolar solvent, the Kasha–Vavilov rule is not fully obeyed. A scheme was constructed in which two ESIPT processes are effective, one starting at the S_1 and the other at the S_2 state, which can explain this rare phenomenon.

Acknowledgment. The research visits of A.S.-H. to LCVU Amsterdam were supported by the European Commission (Integrated Infrastructure Initiative Program, Contract No. RII-CT-2003-506350).

References and Notes

- Zyss, J.; Chemia, D. S.; Nicoud, J. F. *J. Chem. Phys.* **1981**, *74*, 4800–4811.
- Youssif, S. *ARKIVOC* **2001**, 242–268.
- Berdys, J.; Makowski, M.; Makowska, M.; Puszko, A.; Chmurzyński, L. *J. Phys. Chem. A* **2003**, *107*, 6293–6300.
- Szemik-Hojniak, A.; Głowiak, T.; Deperasińska, I.; Puszko, A.; Talik, Z. *Nonlinear Opt., Quantum Opt.* **2003**, *30*, 215.
- Szemik-Hojniak, A.; Głowiak, T.; Deperasińska, I.; Puszko, A. *J. Mol. Struct.* **2001**, *597*, 279–291.
- Szemik-Hojniak, A.; Głowiak, T.; Puszko, A.; Talik, Z. *J. Mol. Struct.* **1998**, *449*, 77–90.
- Kownacki, K.; Mordzinski, A.; Wilbrandt, R.; Grabowska, A. *Chem. Phys. Lett.* **1994**, *227*, 270–276.
- Douhal, A.; Sanz, M.; Carranza, M. A.; Organero, J. A.; Santos, L. *Chem. Phys. Lett.* **2004**, *395*, 387; **2004**, *394*, 54–60.
- Bader, A. N.; Pivovarenko, V. G.; Demchenko, A. P.; Ariese, F.; Gooijer, C. *Spectrochim. Acta, Part A* **2003**, *59*, 1593–1603.
- Klymchenko, A. S.; Pivovarenko, V. G.; Demchenko, A. P. *Spectrochim. Acta, Part A* **2003**, *59*, 787–792.
- Foster, K. L.; Baker, S.; Brousmiche, D. W.; Wan, P. J. *Photochem. Photobiol.*, **A** **1999**, *129*, 157–163.
- Tokomura, K.; Watanabe, Y.; Itoh, M. *Chem. Phys. Lett.* **1984**, *111*, 379–382.
- Bulska, H.; Grabowska, A.; Pakuła, B.; Sepiół, J.; Waluk, J.; Wild, U. P. *J. Lumin.* **1984**, *29*, 65–81.
- Douhal, A.; Kim, S. K.; Zewail, A. H. *Nature* **1995**, *378*, 260–263.
- Chou, P. T.; Wu, G. R.; Wei, C. Y.; Shiao, M. Y.; Liu, Y. I. *J. Phys. Chem. A* **2000**, *104*, 8863–8871.
- Poór, B.; Michniewicz, N.; Kállay, M.; Buma, W. J.; Kubinyi, M.; Szemik-Hojniak, A.; Deperasińska, I.; Puszko, A.; Zhang, H. *J. Phys. Chem. A* **2006**, *110*, 7086–7091.
- Szemik-Hojniak, A.; Deperasińska, I.; Jerzykiewicz, L.; Sobota, P.; Hojniak, M.; Puszko, A.; Haraszkiwicz, N.; van der Zwan, G.; Jacques, P. *J. Phys. Chem. A* **2006**, *110*, 10690–10698.
- Berlman, I. B. *Handbook of Fluorescence Spectra of Aromatic Molecules*; Academic Press: New York, 1971.
- Ingham, K. C.; Abu-Elgheit, M.; Ashraf El-Bayoumi, M. *J. Am. Chem. Soc.* **1971**, *93*, 5023–5025.
- Turro, N. J. *Modern Molecular Photochemistry*; Benjamin/Cummings: Menlo Park, CA, 1978; p 105.
- Valeur, B. *Molecular Fluorescence: Principles and Applications*; Wiley: New York, 2002; p 58.